Channel Aware Routing in MANETs with Route Handoff

Xiaoqin Chen, Haley M. Jones, and Dhammika Jayalath, *Senior Member, IEEE*

Abstract—In wireless mobile ad hoc networks (MANETs), packet transmission is impaired by radio link fluctuations. This paper proposes a novel channel adaptive routing protocol which extends the Ad-hoc On-Demand Multipath Distance Vector routing protocol (AOMDV) to accommodate channel fading. Specifically, the proposed Channel Aware AOMDV (CA-AOMDV) uses the channel average non-fading duration as a routing metric to select stable links for path discovery, and applies a preemptive handoff strategy to maintain reliable connections by exploiting channel state information. Using the same information, paths can be reused when they become available again, rather than being discarded. We provide new theoretical results for the downtime and lifetime of a live-die-live multiple path system, as well as detailed theoretical expressions for common network performance measures, providing useful insights into the differences in performance between CA-AOMDV and AOMDV. Simulation and theoretical results show that CA-AOMDV has greatly improved network performance over AOMDV.

Index Terms—Mobile ad hoc networks, routing protocols, channel adaptive routing.

1 Introduction

Wireless mobile ad hoc networks (MANETs) are self-configuring, dynamic networks in which nodes are free to move. A major performance constraint comes from path loss and multipath fading [1]. Many MANET routing protocols exploit multihop paths to route packets. The probability of successful packet transmission on a path is dependent on the reliability of the wireless channel on each hop. Rapid node movements also affect link stability, introducing a large Doppler spread, resulting in rapid channel variations [2].

Routing protocols can make use of prediction of channel state information (CSI) based on *a priori* knowledge of channel characteristics, to monitor instantaneous link conditions. With knowledge of channel behaviour, the best links can be chosen to build a new path, or switch from a failing connection to one with more favorable channel conditions. Several channel adaptive schemes that have been developed for MANETs to maintain connection stability can be found in the literature. In [3], [4] channel adaptive schemes are implemented in medium access control (MAC) protocols; [5] considers link stability largely in terms of longevity of a given link, termed "associativity"; a similar idea, with respect to node mobility, is considered in [6] while [7] considers node mobility to improve path reliability, utilising only the naive transmission range channel model, not taking into account the fading characteristics of the wireless channel; [8] utilises node-to-node routing, based on the "best" node which received a given transmission. While throughput improvements of 35% over traditional routing techniques are achieved, it is not clear how much delay or overhead is expended through node negotiation with each transmission. [9] uses signal strength as a path selection criterion; [10] introduces outage probability into both the routing and MAC protocols; [11], [12], [13] utilize the bit transmission rate in the network layer; and [14] employs SNR to support channel adaptive routing.

In this paper, we introduce an enhanced, channel-aware version of the AOMDV routing protocol. The key aspect of this enhancement, which is not addressed in other work, is that we use specific, timely, channel quality information allowing us to work with the ebb-and-flow of path availability. This approach allows reuse of paths which become unavailable for a time, rather than simply regarding them as useless, upon failure, and discarding them. We utilise the channel average non-fading duration (ANFD) as a measure of link stability, combined with the traditional hop-count measure for path selection. The protocol then uses the same information to predict signal fading and incorporates path handover to avoid unnecessary overhead from a new path discovery process. The average fading duration (AFD) is utilised to determine when to bring a path back into play, allowing for the varying nature of path usability instead of discarding at initial failure. This protocol provides a dual-attack for avoiding unnecessary route discoveries, predicting path failure leading to handoff and then bringing paths back into play when they are again available, rather than simply discarding them at the first sign of a fade. Further, the same information is required to determine ANFD, AFD and predict

- *X. Chen was with the National ICT Australia and affiliated with the Australian National University at the time of writing. She is now with Star Intellect Pty Ltd, Melbourne Victoria 3000, Australia. E-mail: schen@starintellect.com*
- *H. M. Jones is with the College of Engineering and Computer Science, The Australian National University, Canberra ACT 0200, Australia. E-mail: Haley.Jones@anu.edu.au*
- *D. Jayalath is with the Faculty of Built Environment and Engineering, Queensland University of Technology, Queensland, Australia. E-mail: dhammika.jayalath@qut.edu.au*

path failure, enhancing efficiency. The overall effect is a protocol with improved routing decisions leading to a more robust network. Improvements in performance over AOMDV are around 25% for standard network performance measures. We call this protocol Channel-Aware AOMDV (CA-AOMDV). Note that this protocol is intended to improve on AOMDV in conditions where the channel can be reasonably allowed for. In conditions of high channel variability, there is little sense in even attempting channel prediction and other performance improvement methodologies will need to be utilized.

Further, we provide a detailed theoretical analysis of the lifetimes of both protocols and expressions for performance with respect to routing control overhead, throughput and packet delivery ratio. We derive a new expression for the expected lifetime of a live-die-live-again system of multiple fading paths. These expressions allow us to show the superiority of CA-AOMDV over AOMDV, verified by simulations. Theoretical and simulation results are well-matched.

In Section 2 we review AODV and AOMDV. Statistical properties of the mobile-to-mobile channel model are discussed in Section 3. The route discovery and route maintenance processes in CA-AOMDV are presented in Section 4. A detailed theoretical analysis is presented in Section 5 while simulation results are discussed in Section 6 and conclusions in Section 7.

2 Review of AODV and AOMDV

Transmissions via unreliable wireless connections can result in large packet losses. Thus, it makes sense to consider routing protocols which adapt to channel variations. We propose a channel-aware routing protocol which extends the Ad-hoc On-Demand Multipath Distance Vector (AOMDV) routing protocol [15]. We call it CA-AOMDV. AOMDV is, itself, an extension of the Ad-hoc On-Demand Distance Vector (AODV) routing protocol [16]. In this section we review the details of these two predecessor protocols that are useful to our discussion in this paper.

2.1 AODV

AODV is a single-path, on-demand routing protocol. When a source node, n_s, generates a packet for a particular destination node, n_d, it broadcasts a route request (RREQ) packet. The RREQ contains the following fields:

<source IP address,
source sequence number,
broadcast ID,
destination IP address,
destination sequence number,
hop-count>

where the source and *destination IP addresses* remain constant for the lifetime of the network, *source sequence number* is a monotonically increasing indicator of packet "freshness", *destination sequence number* is the last known sequence number for n_d at n_s and *hop-count* is initialised to zero and incremented at each intermediate node which processes the RREQ. A RREQ is uniquely identified by the combination of *source sequence number* and *broadcast ID*. An intermediate node only processes a RREQ if it has not received a previous copy of it. If an intermediate node has a route to n_d with *destination sequence number* at least that in the RREQ, it returns a route reply (RREP) packet, updated with the information that it has. If not, it records the following information: *source IP address*, *source sequence number*, *broadcast ID*, *destination IP address* and *expiration time* for reverse path route entry, and forwards the RREQ to its neighbors.

Like the RREQ, a RREP is only processed on first sighting and is discarded unless it has a greater *destination sequence number* than the previous RREP or the same *destination sequence number* but a smaller *hop-count*. The RREP packet contains the following fields:

<source IP address,
destination IP address,
destination sequence number,
hop-count,
route expiration time>

The *route expiration time* is the time after which the route is considered to have expired and a new route discovery process must be undertaken. n_s sends packets via the first path it hears about. If it receives a later RREP which has either fresher information or a shorter *hop-count*, it swaps to that, discarding the original route information.

When an active route link breaks, a route error (RERR) packet, with sequence number incremented from the corresponding RREP and hop-count of ∞, is sent by the upstream node of the broken link to n_s. Upon receipt of a RERR, n_s initiates a new route discovery process if it still has packets to send to n_d. Nodes also periodically send "hello" messages to neighboring nodes to maintain knowledge of local connectivity.

2.2 AOMDV

The key distinguishing feature of AOMDV over AODV is that it provides *multiple* paths to n_d. These paths are loop-free and mutually link-disjoint. AOMDV uses the notion of *advertised hop-count* to maintain multiple paths with the same *destination sequence number*. In both AODV and AOMDV, receipt of a RREQ initiates a node route table entry in preparation for receipt of a returning RREP. In AODV the routing table entry contains the fields:

<destination IP address,
destination sequence number,
next-hop IP address,
hop-count,
entry expiration time>

where *entry expiration time* gives the time after which, if a corresponding RREP has not been received, the entry is discarded. In AOMDV the routing table entry is slightly modified to allow for maintenance of multiple

entries and multiple loop-free paths. Firstly, *advertised hop-count* replaces *hop-count* and *advertised hop-count* is the maximum over all paths from the current node to n_d, so only one value is advertised from that node for a given *destination sequence number*. Secondly, *next-hop IP address* is replaced by a list of all *next-hop* nodes and corresponding *hop-counts* of the saved paths to n_d from that node, as follows:

<destination IP address,
destination sequence number,
advertised hop-count,
route list: {(next hop IP 1, hop-count 1),
(next hop IP 2, hop-count 2), ...},
entry expiration time>

To obtain link-disjoint paths in AOMDV n_d can reply to multiple copies of a given RREQ, as long as they arrive via different neighbors.

3 Mobile-to-Mobile Channel Model

In MANETs, potentially all nodes are in motion, so it is appropriate to use the *mobile-to-mobile* channel model [17] to characterize the channel between any two nodes. It is practically difficult to find the *relative speeds* between mobile nodes, so this channel model has the advantage of only using the individual node speeds. It incorporates large-scale path loss and small-scale flat fading. For transmission over a distance, d, in the presence of flat fading, the received signal power is exponentially distributed with mean $G_0 d^{-\alpha}$ [18], where G_0 is proportional to the transmitted signal power and α is the propagation loss coefficient, typically between 2 and 4.

3.1 Average Non-Fading Duration

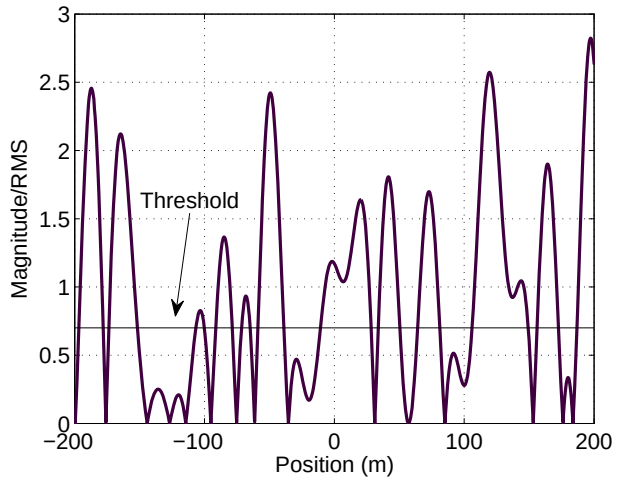

Fig. 1. A typical fading waveform with threshold indicated.

The average non-fading duration (ANFD) is affected by both the physical propagation environment (e.g., obstacles such as trees and buildings) and the node velocities. A typical fading waveform is shown in Fig. 1. The ANFD, $\bar{\vartheta}$, is the average length of time that the signal envelope spends above a network specific threshold, $R_{\rm th}$, and is given by

$$\bar{\vartheta} = \frac{1}{\rho f_T \sqrt{2\pi(1+\mu^2)}} = \frac{c\sqrt{G_0}}{R_{\rm th} d^{\alpha/2} f_0 \sqrt{2\pi(v_T^2+v_R^2)}} \quad (1)$$

where $\rho = R_{\rm th}/R_{\rm rms}$, ($R_{\rm rms} = \sqrt{G_0 d^{-\alpha}}$) is the ratio between the transmission threshold and the root mean square power of the received signal, $f_T = f_0 v_T/c$ is the maximum Doppler shift of the transmitter, f_0 is the transmitter signal carrier frequency, $c \approx 3 \times 10^8 \text{ms}^{-1}$ is the speed of electromagnetic radiation (signal speed), and $\mu = v_R/v_T$ is the ratio of the receiver velocity to that of the transmitter where v_R and v_T are the receiver and transmitter node velocities, respectively.

It can be surmised from (1) that the value of the ANFD is high for low transmission threshold (low ρ), and decreases with an increase of μ or ρ. Further, increased node mobility (captured by v_R and v_T) would cause a corresponding decrease in the ANFD due to the increased rate of signal fluctuations and that an increased link distance (via d) would cause a decrease in ANFD due to a greater path-loss influence.

In MANETs, choice of stable links for route establishment ensures reliable packet transmission. Link stability can be represented by the distance between the nodes forming the link, and their mobilities. Thus, any measure of how stable a link is should include these factors. The ANFD is inversely proportional to link length, d, and node velocities v_T and v_R. The ANFD of a link between two highly mobile or separated nodes will be shorter than that of a link between two slow moving and/or close nodes. In short, a link with a high ANFD will have a relatively long lifetime. Thus, using the ANFD as a metric will result in choosing more stable links. There is minimal extra calculation required to determine ANFD. The parameter $R_{\rm rms}$ can be garnered from received packet signal strengths, and f_T can be calculated via $f_T = f_0 v_T/c$. Thus, to calculate $\bar{\vartheta}$, nodes simply need to include speed and location in the header of each packet.

In this paper we assume that all nodes know their positions and velocities. For example, each node is equipped with a Global Positioning System (GPS) receiver. If it is not feasible to equip every node with a GPS receiver due to availability, node energy limitations, or obstruction of positioning infrastructure, nodes can determine their location by running distributed localization algorithms [19], [20] which only require a limited number of nodes to have position capability. Using received signal strength [21], angle of arrival [22] or time difference of arrival [19], [23], position techniques measure the distance or angle between a node and some known reference points, to estimate location. Similarly, each node is assumed to be able to monitor its velocity by any suitable mechanism [24], [25].

3.2 Average Fading Duration

The average fading duration (AFD), $\bar{\chi}$, is the average length of time that the signal envelope spends below R_{th}. Transmission is not considered possible while the signal envelope for a link is below the threshold. The AFD for the mobile-to-mobile channel is given by [17]

$$\bar{\chi} = \frac{e^{\rho^2} - 1}{\rho f_T \sqrt{2\pi(1+\mu^2)}}. \tag{2}$$

The AFD metric is used in CA-AOMDV to determine for how long a faded link will be unavailable and is recorded in the route cache. This will be discussed in detail in Section 4.2.

3.3 Channel Prediction Using Time Correlation

A feature of CA-AOMDV is the use of channel prediction to instigate handoff between paths, when a fade is predicted on a link on the active path, described in Section 4.2. We choose the linear minimum mean square error (LMMSE) algorithm [26] for channel prediction. We assume a slow fading channel such that it is constant for a symbol duration.

Let M be the number of previously received values used to predict, at discrete time interval n with a discrete time step of Δt, the signal strength ψ time intervals into the future. Then, if $\hat{x}(n+\psi)$ is the LMMSE prediction for the received signal strength, $x(n+\psi)$, at discrete time $n+\psi$, we have

$$\hat{x}(n+\psi) = \mathbf{R}_{\hat{x}x}^T \mathbf{R}_{xx}^{-1} \mathbf{x} \tag{3}$$

where $\mathbf{R}_{\hat{x}x}^T$ is the $1 \times M$ cross-correlation vector of $\hat{x}$ and $\mathbf{x}$, $(\cdot)^T$ denotes transpose, $\mathbf{R}_{xx}$ is the $M \times M$ auto-correlation matrix of $\mathbf{x} = [x(n-1), x(n-2), \cdots, x(n-M)]^T$, and $\mathbf{x}$ is the $M \times 1$ vector of the M previous signal strength values. The auto-correlation matrix $\mathbf{R}_{xx}$ is given by

$$\mathbf{R}_{xx} = \begin{bmatrix} R_{xx}(1,1) & R_{xx}(1,2) & \cdots & R_{xx}(1,M) \\ R_{xx}(2,1) & R_{xx}(2,2) & \cdots & R_{xx}(2,M) \\ \vdots & \vdots & \cdots & \vdots \\ R_{xx}(M,1) & R_{xx}(M,2) & \cdots & R_{xx}(M,M) \end{bmatrix} \tag{4}$$

where element $R_{xx}(\ell, m)$ is given by [17].

$$\begin{aligned} R_{xx}(\ell,m) &= E\{x(n-\ell)x^H(n-m)\} \\ &= \sigma_1^2 J_0(2\pi f_T(m-\ell)) J_0(2\pi f_R(m-\ell)) \end{aligned} \tag{5}$$

where $(\cdot)^H$ denotes Hermitian transpose, $\sigma_1 = R_{\text{rms}}/\sqrt{2}$ and J_0 is the 0^{th} order Bessel function of the first kind. Finally,

$$\mathbf{R}_{\hat{x}x}^T = [R_{\hat{x}x}(1), R_{\hat{x}x}(2) \cdots R_{\hat{x}x}(M)]$$

where

$$\begin{aligned} R_{\hat{x}x}(m) &= E\{\hat{x}(n+\psi)x^H(n+\psi-m)\} \\ &= \sigma_1^2 J_0(2\pi f_T m) J_0(2\pi f_R m). \end{aligned} \tag{6}$$

With the presence of Bessel functions, the LMMSE algorithm is computationally intensive. To enhance amenability to MANET channel prediction, (3) can be reduced as follows.

$$\begin{aligned} \hat{x}(n+\psi) &= (\mathbf{R}_{\hat{x}x}^T \mathbf{R}_{xx}^{-1})\mathbf{x} = \mathbf{W}\mathbf{x} \\ &= [w(1) \cdots w(M)][x(n-1) \cdots x(n-M)]^T \\ &= \sum_{i=1}^{M} w(i)x(n-i) \end{aligned} \tag{7}$$

where $\mathbf{W} = (\mathbf{R}_{\hat{x}x}^T \mathbf{R}_{xx}^{-1})$ with elements $w(i)$, $\{i = 1, \cdots, M\}$. The $w(i)$ values can be calculated off-line and stored in a lookup table indexed by Doppler frequency shift and discrete time shift. The use of this low-complexity LMMSE prediction in CA-AOMDV handoff is discussed in Section 4.2.

4 Channel-Aware AOMDV Protocol

As mentioned in Section 2, route discovery in AOMDV results in selection of multiple loop-free, link-disjoint paths between n_s and n_d, with alternative paths only utilized if the active path becomes unserviceable. One of the main shortcomings of AOMDV is that the only characteristic considered when choosing a path is the number of hops. Path stability is completely ignored. Thus, selected paths tend to have a small number of long hops meaning that nodes are already close to the maximum possible communication distance apart, potentially resulting in frequent link disconnections. Further, channel conditions are idealized with the path-loss/transmission range model, ignoring fading characteristics inherent in all practical wireless communication environments.

In CA-AOMDV, we address this deficiency in two ways. In the route discovery phase we utilise the ANFD, defined in Section 3.1, of each link as a measure of its stability. In the route maintenance phase, instead of waiting for the active path to fail, we pre-empt a failure by using channel prediction on path links, allowing a handover to one of the remaining selected paths. This results in saved packets and consequently smaller delays.

4.1 Route Discovery in CA-AOMDV

Route discovery in CA-AOMDV is an enhanced version of route discovery in AOMDV, incorporating channel properties for choosing more reliable paths. In Section 3.1, we defined the ANFD for one link of a path, according to the mobile-to-mobile channel model. CA-AOMDV uses the ANFD as a measure of link lifetime. The duration, $\mathcal{D}$, of a path is defined as the minimum ANFD over all of its links,

$$\mathcal{D} \triangleq \min_{1 \le h \le \mathcal{H}} \text{ANFD}_h, \tag{8}$$

where h is link number, and $\mathcal{H}$ is number of links/hops in the path. Before forwarding a RREQ to its neighbors, a node inserts its current speed into the RREQ header so that its neighbors can calculate the link ANFD using (1). The path duration, $\mathcal{D}$, is also recorded in the RREQ, updated, as necessary, at each intermediate node. Thus,

TABLE 1
Comparison of routing table entry structures in AOMDV and CA-AOMDV.

AOMDV routing table	CA-AOMDV routing table
destination IP address	destination IP address
destination sequence number	destination sequence number
advertised hop-count	advertised hop-count
	$\mathcal{D}_{\min}$
path list {(next hop IP 1,hop-count 1), (next hop IP 2,hop-count 2),$\cdots$}	path list {(next hop 1,hop-count 1,$\mathcal{D}_1$), (next hop 2,hop-count 2,$\mathcal{D}_2$),$\cdots$}
	expiration timeout
expiration timeout	handoff dormant time

all information required for calculating the ANFD is available via the RREQs, minimizing added complexity.

Similarly to the way the longest hop path is advertised for each node in AOMDV to allow for the worst case at each node, in CA-AOMDV the minimum $\mathcal{D}$ over all paths between a given node, n_i, and n_d, is used as part of the cost function in path selection. That is,

$$\mathcal{D}_{\min}^{i,d} \triangleq \min_{\zeta \in \text{path\_list}_i^d} \mathcal{D}_\zeta \tag{9}$$

where path_list_i^d is the list of all saved paths between nodes n_i and n_d. The route discovery update algorithm in CA-AOMDV is a slight modification of that of AOMDV. If a RREQ or RREP for n_d at n_i, from a neighbor node, n_j, has a higher *destination sequence number* or shorter *hop-count* than the existing route for n_d at n_i, the route update criterion in CA-AOMDV is the same as that in AOMDV. However, if the RREQ or RREP has a *destination sequence number* and *hop-count* equal to the existing route at n_i but with a greater $\mathcal{D}_{\min}^{i,d}$, the list of paths to n_d in n_i's routing table is updated.

So, in CA-AOMDV, path selection is based on $\mathcal{D}_{\min}^{i,d}$ as well as *destination sequence number* and *advertised hop-count*. The routing table structures for each path entry in AOMDV and CA-AOMDV are shown in Table 1. The *handoff dormant time* field in the routing table for CA-AOMDV is the amount of time for which the path should be made dormant due to channel fading. It is set to the maximum value of the AFDs over all links in the path. This use of *handoff dormant time* is described in more detail in the next section.

4.2 Route Maintenance in CA-AOMDV

In mobile environments, it is necessary to find efficient ways of addressing path failure. Using prediction and handoff to preempt fading on a link on the active path, disconnections can be minimized, reducing transmission latency and packet drop rate [27], [28].

Route maintenance in CA-AOMDV takes advantage of a handoff strategy using signal strength prediction, detailed in Section 3.3, to counter channel fading. When the predicted link signal strength level falls below a network-specific threshold, the algorithm swaps to a good-quality link. The fading threshold is chosen so as to provide robustness to prediction errors. The presence of multiple users experiencing independent channel fading means that MANETs can take advantage of channel diversity, unlike data rate adaptation mechanisms such as SampleRate [29].

All nodes maintain a table of past signal strengths, recording for each received packet, *previous hop*, *signal power* and *arrival time*. Ideally there will be M packets where M is the required number of past samples from (3). However, this will depend on the packet receipt times compared with the specified discrete time interval, Δt. If packets are received at time intervals greater than Δt, sample signal strengths for the missed time intervals can be approximated by the signal strength of the packet closest in time to the one missed. If packets are received at intervals of shorter duration than Δt, some may be skipped. An example of handoff in CA-AOMDV is shown in Fig. 2. The handoff process is implemented via a handoff request (HREQ) packet. The CA-AOMDV handoff scheme is described below.

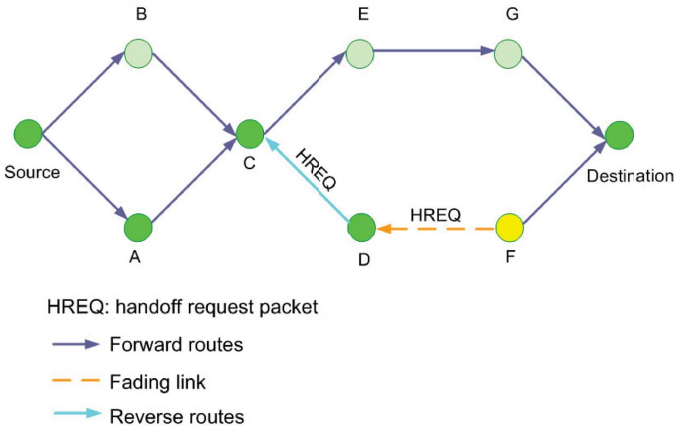

Fig. 2. Handoff in CA-AOMDV. Node F has predicted a forthcoming fade for its link with node D and has generated a HREQ. Having no alternative paths to choose from, node D forwards the HREQ to node C which may then be able to handoff to the path with node E as the next node.

4.2.1 Prediction Length

The LMMSE prediction algorithm performs quite poorly if not matched to the current channel conditions. Therefore, the prediction length should not be too long. In CA-AOMDV a given node may have multiple paths to the destination, each with a different next hop node. If an intermediate node has multiple paths to the destination, upon receiving an HREQ it can immediately switch from the active path to a good alternative one, without further propagating the HREQ. Therefore, the time needed to implement a handoff in CA-AOMDV is the duration, in terms of the discrete time interval Δt, for the HREQ to be propagated to the fading link uplink node. For example, if n_i and n_j are neighbors in a given path and n_j predicts a fade on link $\ell_{i,j}$, it will generate a HREQ and forward it to n_i. Thus, a suitable prediction

length ψ in (3) corresponds to the number of discrete time intervals, Δt, for transmission of a HREQ between n_j and n_i, which can be approximated by using the data propagation time T_j^i from n_j to n_i, with

$$\psi = \text{round}(T_j^i/\Delta t). \tag{10}$$

where "round" is the integer rounding function. In addition to choosing a threshold with a suitable error margin, as described above, to enhance the robustness of the prediction process to errors in CA-AOMDV the signal strength is predicted at $t_0 + \psi$ and $t_0 + 2\psi$. The algorithm is detailed in the next section.

4.2.2 Handoff Trigger

Route handoff is triggered when a link down-stream node predicts a fade and transmits a HREQ to the up-link node. Let T_R be the transmission range, assumed to be the same for all nodes, let $\hat{R}(t)$ be predicted signal strength at time t and recall R_{th} as the fade prediction threshold. If the prediction at $t_0 + \psi$ is above R_{th} while that at $t_0+2\psi$ is below, the maximum transmitter velocity $v_T^{\max}$ ensuring signal strength above R_{th} at $t_0 + \psi$, is determined using (3). If a fade is predicted at either time, the receiver checks whether the link is at breaking point with respect to distance. The HREQ registers the following fields: *source IP address*, *destination IP address*, *source sequence number*, *fade interval index*, *long term fading indicator*, *AFD* and $v_T^{\max}$.

4.2.3 Handoff Table to Avoid Duplicate HREQs

In addition to the routing table described in Table 1, each node maintains a local handoff table. Each entry includes: *source IP address*, *source sequence number*, *destination IP address* and *expiration timeout*. *expiration timeout* indicates when a path is expected to be available again (out of the fade) and is set to the maximum AFD of all currently faded links with paths through that node to a particular n_s. Note that this is similar to the way *advertised hop-count* is set to the maximum number of hops for any path going through a node for a particular n_s in AOMDV. Whenever a node receives a HREQ targeting a particular n_s, it checks its handoff table for an entry relating to that n_s. The handoff table is updated if no entry exists for that n_s, if the new HREQ has a longer AFD or if the existing entry is stale due to the *expiration timeout* having expired. If any unexpired entry is found for that n_s with the same or higher *source sequence number*, the HREQ is dropped.

4.2.4 Forwarding the HREQ

Any node receiving a non-duplicate HREQ checks for alternative paths to n_d. If not, as for the case of node D in Fig. 2, it propagates the HREQ. Otherwise, if it has one or more "good" alternative paths to the n_d, it marks the fading path indicated in the HREQ as dormant, setting the *handoff dormant time* in its routing table entry for that path to the AFD recorded in the HREQ. The HREQ is then dropped. If a fade is predicted on the active path, a nondormant alternative path to n_d is then adopted prior to the onset of link failure. For example, if node C in Fig. 2 receives a HREQ from node D, it marks the path with *next hop* = D as dormant, and adopts the path with *next hop* = E. The dormant path is retained for use when the fade is over, reducing path discovery overhead.

Section Summary:

- **Route discovery:** ANFD is combined with the hop-count criterion from AOMDV to serve as a metric with which to select short but stable paths instead of simply choosing the shortest path. So, CA-AOMDV takes into account stability and length to improve overall path quality.
- **Route maintenance:** Assuming independently time-varying paths, CA-AOMDV uses predicted signal strength to trigger a handoff before a fade occurs, reducing the n_s-n_d connection failure rate. The breaking link AFD is recorded, so that it may be reutilized once out of the fade.

5 Theoretical Analysis

A framework is now presented to analyze the performances of AOMDV and CA-AOMDV. The probability density functions (PDFs) of the lifetimes of a single path and multiple paths are derived and the performances in terms of routing control overhead and network throughput are analyzed.

5.1 Network Model

Assume an N-node network uniformly distributed over an area of side length $2S$. The node density is $\sigma = N/(2S)^2$ per m^2. The number of connections in the network is C. Assuming all nodes in the network have equal transmission range, T_R, the average number of neighbors is $n = \sigma\pi T_R^2 - 1$. The expected distance between a n_s-n_d pair for each connection is $\frac{S}{3}(\sqrt{2} + \ln(1 + \sqrt{2}))$ [30], so we can approximate the expected number of hops $\hat{\mathcal{H}}$ per connection by

$$\hat{\mathcal{H}} = \frac{S(\sqrt{2} + \ln(1 + \sqrt{2}))}{3T_R}. \tag{11}$$

Assume each path link has equal likelihood of being broken at any time. On average, the number of hops into a connection (path) before encountering a broken link is $(\hat{\mathcal{H}} + 1)/2$. The average number of active links at any given time is $C\hat{\mathcal{H}}$, and the total number of network links is approximately $nN/2$, so the average number of connections over a given link is

$$B = \frac{2C\hat{\mathcal{H}}}{(n+1)N}. \tag{12}$$

5.2 Single Path Lifetime Statistics

Link lifetime is the length of time for which a link is "active". It is affected by the movements of the pair of linked nodes and the channel fading characteristics. If only free-space propagation is considered, link lifetime is simply the amount of time for which the two nodes are within each other's transmission ranges. If channel fading is also considered the relationship between link lifetime and distance is not so straightforward, as the fading component is independent of distance.

We use the random variable (r.v.) Z_ℓ to represent the lifetime of a fading link, which is equal to the non-fading duration of the link, from (1). It is most commonly modelled by an exponential distribution. We therefore assume that the lifetime for link ℓ has PDF, $f_{Z_\ell}(t) = \lambda_\ell e^{-\lambda_\ell t}$.

As discussed in Section 2, the multiple cached paths at a given n_s for a given n_d are link-disjoint in AOMDV. Thus, we assume that the lifetimes of the links of the multiple cached paths are independent. While this is not strictly the case, here we are seeking general trends, and this approximation is, therefore, appropriate. For a path composed of L fading links, path lifetime can be represented by $Z_p = \min[Z_1, \cdots, Z_L]$, where Z_ℓ, $\{\ell = 1, \cdots, L\}$, represents the exponentially distributed r.v. for the lifetime of link ℓ with parameter λ_ℓ. It can be shown that the CDF $F_{Z_p}(t)$ of Z_p is given by [31]

$$F_{Z_p}(t) = 1 - e^{-\left(t\Sigma_{\ell=1}^{L}\lambda_\ell\right)}, \tag{13}$$

and the PDF,

$$f_{Z_p}(t) = e^{-t\sum_{k=1}^{L}\lambda_k}\sum_{\ell=1}^{L}\lambda_\ell = \lambda_p e^{-\lambda_p t} \tag{14}$$

where $\lambda_p = \sum_{\ell=1}^{L}\lambda_\ell$. If all L links are independent and identically distributed (i.i.d.) with parameter λ, then (14) becomes

$$f_{Z_p}(t) = L\lambda e^{-L\lambda t}. \tag{15}$$

Using (14), the expected path lifetime is, then

$$\mathrm{E}\{Z_p\} = \int_0^\infty t\lambda_p e^{-\lambda_p t}dt = \frac{1}{\lambda_p} = \frac{1}{\sum_{\ell=1}^{L}\lambda_\ell} \tag{16}$$

and $1/\lambda_p = 1/L\lambda$ for L i.i.d. links in a path. So, a path with L i.i.d. links has a lifetime L times less than any individual link, on average.

5.3 Multiple Path Lifetime in AOMDV

To analyse the active lifetimes of the multiple path systems in AOMDV and CA-AOMDV, we assume N_p paths are established during route discovery. In order to enable meaningful comparisons between the two schemes, we also assume that each path has exactly L links and that the individual link lifetimes are exponentially i.i.d. with parameter λ for $Z_\ell, \{\ell = 1, \ldots, L\}$.

Assume that at time t path p_1 is the active path in an AOMDV network. When p_1 fails, n_s attempts to adopt an alternative path, and p_1 is discarded from the cache. Communication between n_s and n_d is broken when all N_p paths have failed. Let Z_A be the r.v. representing the lifetime of the multiple path system in AOMDV and let Z_{p_i} be the r.v. representing the lifetime of path p_i with parameter $\lambda_p = L\lambda$. Using (13) and (14), the probability that all paths have failed at time t is the CDF of Z_A, given by

$$\begin{aligned}\Pr\{Z_A < t\} &= \mathrm{P_r}\{(Z_{p_1} < t) \cap (Z_{p_2} < t) \cap \cdots \cap (Z_{p_{N_p}} < t)\} \\ &= \prod_{i=1}^{N_p}\mathrm{P_r}\{Z_{p_i} < t\} = \prod_{i=1}^{N_p}F_{Z_{p_i}}(t) \\ &= (1 - e^{-\lambda_p t})^{N_p}. \end{aligned} \tag{17}$$

Taking the derivative of (17), gives the PDF of Z_A

$$f_{Z_A}(t) = N_p\lambda_p\sum_{k=0}^{N_p-1}(-1)^{N_p-k-1}\left(\begin{array}{c} N_p-1 \\ k \end{array}\right)e^{-(N_p-k)\lambda_p t} \tag{18}$$

and the expected value of Z_A is given by

$$\mathrm{E}\{Z_A\} = \frac{N_p}{\lambda_p}\sum_{k=0}^{N_p-1}(-1)^{N_p-k-1}\left(\begin{array}{c} N_p-1 \\ k \end{array}\right)\frac{1}{(N_p-k)^2}. \tag{19}$$

5.4 Multiple Path Downtime in CA-AOMDV

Handoff is adopted in CA-AOMDV to enable swapping between alternative paths when a fade is predicted on the active path. At time t, let path p_1 be the active path. When p_1 fails, it is marked as dormant for the predicted period of its fade and p_2 is made active, and so on. The difference from AOMDV is that any path recovering from a fade can again be considered for active use. So, with CA-AOMDV, a new route discovery process is only required when all N_p paths are *simultaneously* in a fade. So, we need to know how often this happens, or how long the multiple path system "downtime" is for multiple reselectable paths.

Now, because, in CA-AOMDV the system is active if any path is active at any time, but "disconnected" only if all paths are "down" (faded) simultaneously, we start with expressions for the system downtime and then determine the system lifetime in terms of the system downtime. We start at the link level. Similarly to the link lifetime (non-fading duration), the link downtime (fading duration) has an exponential distribution. Remembering that all links are i.i.d., let the r.v. Y_ℓ represent the downtime of link ℓ, with parameter γ, with CDF $F_{Y_\ell}(t) = 1 - e^{-\gamma t}$. Also let the r.v. Y_p represent the downtime of path p, with parameter γ_p, with CDF, $F_{Y_p}(t)$. Finally, let the r.v. Y_C represent the multiple path system downtime for CA-AOMDV, with CDF, $F_{Y_C}(t)$. The CA-AOMDV system is down only when all paths are down, which occurs when at least one link in each path is down. So, the probability that the CA-AOMDV

system is down at time t is

$$\Pr\{Y_C > t\} = \prod_{i=1}^{N_p} \Pr\{Y_{p_i} > t\} = \prod_{i=1}^{N_p} \left(1 - \prod_{\ell=1}^{L} \Pr\{Y_\ell < t\}\right) = \prod_{i=1}^{N_p} \left(1 - \prod_{\ell=1}^{L} F_{Y_\ell}(t)\right) = \left[1 - \left(1 - e^{-\gamma t}\right)^L\right]^{N_p} \tag{20}$$

Then the CDF of Y_C is given by

$$F_{Y_C}(t) = 1 - \left[1 - \left(1 - e^{-\gamma t}\right)^L\right]^{N_p}. \tag{21}$$

Then, taking the derivative of (21), the PDF of the CA-AOMDV multiple path system downtime, Y_C, with i.i.d. links is given by (22) and the expected downtime of the CA-AOMDV multiple path system is given by (23).

5.5 Multiple Path Lifetime in CA-AOMDV

In a fading channel, the AFD is given by the quotient of the probability of a fade and the level crossing rate (LCR), where the LCR is the rate in times per second that the signal amplitude in the channel crosses a given threshold in the positive going direction. Similarly, the ANFD is given by the quotient of the probability of not being in a fade and the LCR. Then, the ANFD in terms of the AFD, is

$$\text{ANFD} = \frac{\Pr(\text{not in fade})}{\text{LCR}} = \frac{1 - \Pr(\text{in fade})}{\Pr(\text{in fade})}\text{AFD} \tag{24}$$

For a multiple path system, the AFD is analogous to the system downtime and the ANFD is analogous to the system lifetime. So, for CA-AOMDV, we substitute (23) for the AFD in (24). We need to determine an expression for the probability that the CA-AOMDV system is "in a fade", or "down". Now, the probability that the CA-AOMDV multiple path system is down is the probability that all paths are down. The probability that any particular path is down is the probability that at least one link in the path is undergoing a fade. In [32] it was shown that the signal envelope of a mobile-to-mobile signal has a Rayleigh distribution. Recall the Rayleigh parameter, ρ, from Section 3.1. The probability that the CA-AOMDV system, with N_p paths each with L i.i.d. links, is in a fade is given by

$$\Pr(\text{system in fade}) = \prod_{i=1}^{N_p} \left(1 - \prod_{\ell=1}^{L} e^{-\rho^2}\right) = \left(1 - e^{-L\rho^2}\right)^{N_p} \tag{25}$$

Then, letting Z_C be the r.v. representing the CA-AOMDV system lifetime and combining (23), (24) and (25), the average system lifetime for CA-AOMDV is given by

$$E\{Z_C\} = \frac{1 - \left(1 - e^{-L\rho^2}\right)^{N_p}}{\left(1 - e^{-L\rho^2}\right)^{N_p}} E\{Y_C\}. \tag{26}$$

This new theoretical result allows us to compare the theoretical lifetimes of multiple path systems with and without reuse.

5.6 System Lifetime Comparison

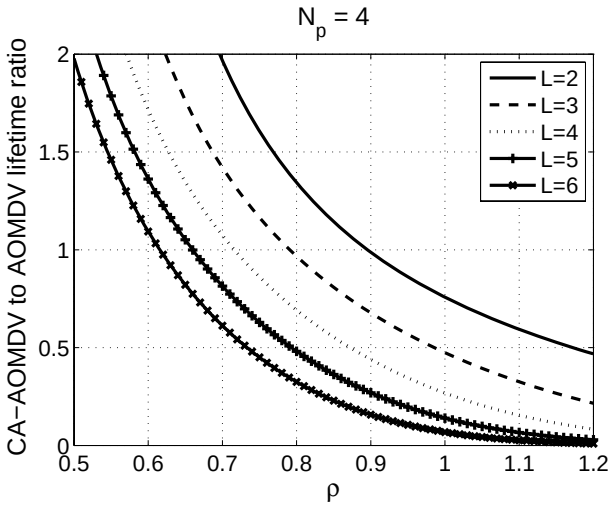

Fig. 3. Ratio of multiple path system lifetime for CA-AOMDV to AOMDV for increasing values of link fading threshold parameter ρ.

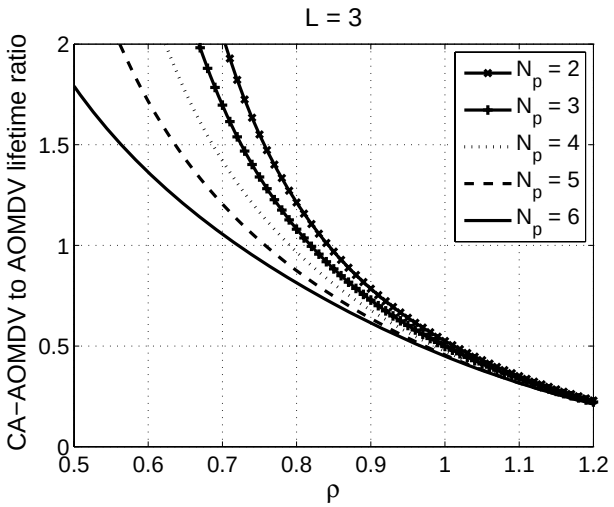

Fig. 4. Ratio of multiple path system lifetime for CA-AOMDV to AOMDV for increasing values of link fading threshold parameter ρ.

In Figures 3 and 4, we show the ratio of the multiple path system lifetimes in CA-AOMDV to AOMDV with four paths and varying numbers of links per path, and varying numbers of paths with three links, as it varies with link Rayleigh fading threshold parameter ρ. The ratios are calculated from dividing (26) by (19). Note that the more paths there are, the better the performance of either system and the more links there are, the worse the performance. The ratio of system lifetime for CA-AOMDV over AOMDV increases exponentially as the fading threshold, ρ, decreases. Recall that ρ is the ratio of the signal fading threshold to the link RMS signal strength. So, the higher the value of ρ, the higher the signal strength must be for the link to be considered *not*

$$f_{Y_C}(t) = \gamma N_p L \sum_{k=0}^{N_p-1} (-1)^{N_p-k-1} \binom{N_p-1}{k} \sum_{i=0}^{L(N_p-k)-1} (-1)^{L(N_p-k)-1-i} \binom{L(N_p-k)-1}{i} e^{-[L(N_p-k)-i]\gamma t} \quad (22)$$

$$E\{Y_C\} = \frac{N_p L}{\gamma} \sum_{k=0}^{N_p-1} (-1)^{N_p-k-1} \binom{N_p-1}{k} \sum_{i=0}^{L(N_p-k)-1} (-1)^{L(N_p-k)-1-i} \binom{L(N_p-k)-1}{i} \frac{1}{(L[N_p-k]-i)^2}. \quad (23)$$

in a fade. The ratio improves with a decrease in number of paths and a decrease in number of links per path. That is, while the actual lifetimes improve with more paths and fewer links, the advantage of CA-AOMDV over AOMDV improves with fewer paths and fewer links. This makes sense because taking the channel into account, as in CA-AOMDV, becomes more complex and less effective with more channels (links) to consider.

Fig. 5 shows the theoretical and simulated multiple path system lifetimes for CA-AOMDV and AOMDV for $N_p = 2$ paths and $L = 2$ links. The theoretical values are from (19) and (26). The simulation values were generated in Matlab using a scenario with 20 scattering points outside a network area of $1000 \times 20\text{m}^2$ with a transmission wavelength of 0.3m (∼1GHz). Adding the signals from each scattering point at each point of interest in the network results in a Rayleigh distributed wavefield. The resolution of points at which signal strength values were taken was 1mm. At low lifetime distances, the simulation results are limited by this resolution. It can be seen that the simulated and theoretical results are in excellent agreement, particularly for lower values of ρ. CA-AOMDV outperforms AOMDV up until $\rho \approx 0.7$, after which time AOMDV performs better in theory, with no distinction in the simulation results. Further, if we look at the actual lifetime values, by this point they are, at most, 8cm which, even at 20km/hr is only 14ms. Such small lifetimes leave both schemes requiring further enhancements such as signal coding. Note these results also do not take into account the fact that AOMDV chooses paths based only on hop-count, whereas CA-AOMDV includes link quality. Taking these points into account would improve the system lifetime performance of CA-AOMDV even further over that of AOMDV.

Note that $1/\gamma_\ell$ for the AOMDV results in Figures 3, 4 and 5 can be calculated for a given value of ρ by equating it with the right-hand-side of (1) and $1/\gamma$ for the CA-AOMDV results can be calculated for a given value of ρ by equating it with the right-hand-side of (2). For these figures, μ was set to 1, a reasonable assumption, as was f_T. Changing f_T has no effect on Figures 3 and 4 and has a simple scaling effect on the results in Fig. 5.

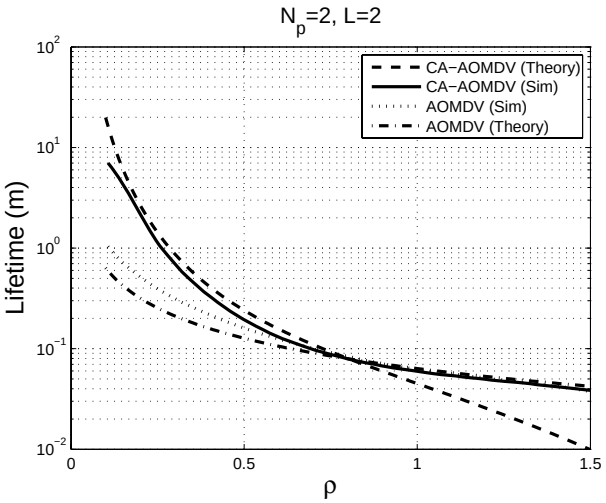

Fig. 5. Theoretical and simulated multiple path system lifetimes, in meters, for $N_p = 2$ and $L = 2$ for CA-AOMDV and AOMDV.

5.7 CA-AOMDV/AOMDV Performance Analysis

We now determine expressions for routing control overhead and packet delivery ratio. If Φ^d is the average delay for a route discovery and $\mathrm{E}\{Z\}$ is the average path system lifetime, from (19) or (26), then $(\mathrm{E}\{Z\} + \Phi^d)$ represents the average time between two successive route discoveries [31] per n_s-n_d pair. Let Ω be the number of route discoveries per second,

$$\Omega = \frac{1}{\mathrm{E}\{Z\} + \Phi^d}. \quad (27)$$

In CA-AOMDV and AOMDV, when n_s needs a path to n_d, it broadcasts a RREQ. n_d, or any intermediate node which has a fresh enough path to n_d, feeds a RREP back to n_s to establish the path. We can approximate Φ^d as

$$\Phi^d = \hat{\mathcal{H}}(t_Q + t_P) \quad (28)$$

where t_Q is the one-hop propagation time of a RREQ, and t_P is the one-hop propagation time of a RREP. With C connections in the network, each lasting an average of T seconds, the average number of route discovery processes over time T is equal to $N_{\mathrm{rd}} = CT\Omega$.

5.7.1 Routing Control Overhead (Υ)

In a multiple path system, the routing control overhead includes replacing the failed path, Υ^r, and route discovery overhead, Υ^d, when all alternative paths are broken. First we consider the routing control overhead introduced by route discovery. The RREQs are flooded into the N-node network, and N_p RREPs are unicast from n_d to n_s, where N_p is the number of multiple paths established during route discovery. So, the routing control overhead over a time T is given by

$$\Upsilon^d = n_{\mathrm{RREQ}} + n_{\mathrm{RREP}} = CT\Omega(N + N_p\hat{\mathcal{H}}) \quad (29)$$

where n_{RREQ} is the number of RREQs, and n_{RREP} is the number of RREPs, generated during the route discovery.

Now we consider the control overhead for path replacement, Υ^r. In each source-destination pair, there are N_p alternative paths, so, there can be at most N_p path repairs. In the event of a path disconnection, the upstream node of the broken link sends a RERR to n_s. If the upstream node has no alternative paths to n_d, and it is located closer to n_d than n_s, it broadcasts a RREQ for n_d to salvage the data packets. (If the broken link is closer to n_s than n_d, any enroute packets are discarded.) Assuming that the link failure is equally likely to happen in any link of the path, the maximum number of path replacements is $CT\Omega_{\mathrm{A}}N_p/2$, where Ω_{A} is the AOMDV route discovery frequency.

So, the routing control overhead due to path failure includes the RERRs triggered by the failed link, the path repair RREQs flooded from the fading link to n_d, and the RREPs from n_d to the RREQ generator. Because only link breaks in the latter half of a path are atoned for, RREQs are flooded into the network over an average of $\hat{\mathcal{H}}/4$ hops, with the average number of flooded RREQs during each path repair approximately being $N_{\mathrm{rq}} = \pi(\hat{\mathcal{H}}R/4)^2\sigma$. The RREPs are unicast from n_d to the RREQ broadcasting node, while the RERRs are unicast from the fading link to n_s. In each path failure, the average number of connected paths over a breaking link is B from (12). The AOMDV routing control overhead due to path failure, Υ^r_{A}, is

$$\Upsilon^r_{\mathrm{A}} = n_{\mathrm{RERR}} + n_{\mathrm{RREQ}} + n_{\mathrm{RREP}} \tag{30}$$

$$n_{\mathrm{RERR}} = [CTN_p\Omega_{\mathrm{A}}B(\hat{\mathcal{H}}+1)]/2 \tag{31}$$

$$n_{\mathrm{RREQ}} = [CTN_p\Omega_{\mathrm{A}}BN_{\mathrm{rq}}]/2 \tag{32}$$

$$n_{\mathrm{RREP}} = [CTN_p\Omega_{\mathrm{A}}B\hat{\mathcal{H}}]/4 \tag{33}$$

where n_{RERR} is the number of RERRs due to path failure, and Ω_{A} is AOMDV average route discovery frequency. The total routing control overhead in AOMDV due to path failure in time T is, from (30), (31), (32), and (33)

$$\Upsilon^r_{\mathrm{A}} = CTN_p\Omega_{\mathrm{A}}B\left(\frac{3\hat{\mathcal{H}}+2}{4} + \frac{N_{\mathrm{rq}}}{2}\right). \tag{34}$$

If the upstream node of the broken link has multiple paths to n_d, it can use an alternative path without propagation of RREQs and RREPs. Under these circumstances, (30) can be simplified to $\Upsilon^r_{\mathrm{A}} = n_{\mathrm{RERR}}$ from (31).

In CA-AOMDV, routing control overhead involves HREQs, terminated at the nearest intermediate nodes having multiple paths to the destinations. The number of handoffs between two successive route discoveries is determined by the channel fading status. However, we can approximate it by N_p. Assuming the expected number of hops to deliver a HREQ is $\hat{\mathcal{I}}$ with $\hat{\mathcal{I}} \le \hat{\mathcal{H}}$, then the CA-AOMDV routing control overhead due to path failure is

$$\Upsilon^r_{\mathrm{C}} = n_{\mathrm{HREQ}} = CTN_p\Omega_{\mathrm{C}}B\hat{\mathcal{I}} \tag{35}$$

where Ω_{C} is the average route discovery frequency in CA-AOMDV. For the case where multiple paths exist in the upstream node of a broken link the CA-AOMDV routing control overhead is just one-hop HREQ propagation with $\hat{\mathcal{I}} = 1$, that is, $\Upsilon^r_{\mathrm{C}} = CTN_p\Omega_{\mathrm{C}}B$. Then, the total routing control overhead is $\Upsilon = \Upsilon^d + \Upsilon^r$, with

$$\Upsilon_{\mathrm{A}} = CT\Omega_{\mathrm{A}}(N + N_p\hat{\mathcal{H}}) + CTN_p\Omega_{\mathrm{A}}B\left(\frac{3\hat{\mathcal{H}}+2}{4} + \frac{N_{\mathrm{rq}}}{2}\right) \tag{36}$$

$$\Upsilon_{\mathrm{C}} = CT\Omega_{\mathrm{C}}(N + N_p\hat{\mathcal{H}}) + CTN_p\Omega_{\mathrm{C}}B\hat{\mathcal{I}} \tag{37}$$

where Ω_{A} and Ω_{C} are the route discovery frequencies for AOMDV and CA-AOMDV, respectively.

We showed in the previous section that the multiple path system lifetime for CA-AOMDV was longer than that for AOMDV, for median to low thresholds with no practical difference at higher thresholds. So the number of route discoveries per second, Ω, is generally smaller for CA-AOMDV than AOMDV. If we also compare the differentiating terms in (36) and (37), it can be shown that $3(\hat{\mathcal{H}}+2)/4 + N_{\mathrm{rq}}/2 > \hat{\mathcal{I}}$, always. Thus, the routing overhead for AOMDV is greater than that for CA-AOMDV as long as the signal threshold is not too high, at which point they are about equal.

5.7.2 Packet Delivery Ratio (Ψ)

The packet delivery ratio is the ratio of the number of successfully received to the number of generated packets. The time, T, for a source-destination connection can be approximately divided into two parts, the path connection time, T_{con}, and the connection delay which is the time to contend for channel access and to reconnect due to channel fading. In a network with constant bit rate sources and constant data rate, we can model the data as being delivered uniformly over time, such that the packets delivered within T_{con} are correctly received, and those delivered during the time of connection delay are incorrectly received. Then, the ratio between the path connection time, T_{con}, and the total operation time, T, can be used to model packet delivery ratio.

The path connection delay, Φ, includes the delay, Φ^r, due to activation of an alternative path, and the delay, Φ^d, from (28), due to route discovery when all alternative paths are broken. In AOMDV, the delay due to alternative path activation is the time to propagate the RERRs back to n_s. Let t_r be the one-hop propagation time of a RERR. The delay due to switching between alternative paths over a time T is, from (31)

$$\Phi^r_{\mathrm{A}} = t_r \times n_{\mathrm{RERR}} = \frac{TN_p\Omega_{\mathrm{A}}t_r(\hat{\mathcal{H}}+1)}{2}. \tag{38}$$

In CA-AOMDV, the connection delay is the HREQ propagation time t_hI. The total connection delay is $\Phi = \Phi^d + \Phi^r$. Thus, the path connection time is $T - \Phi$. For 802.11 DCF, there are also delays incurred for MAC overhead and retransmission. For each data transmission, the minimum channel occupation due to MAC overhead is $T_{\mathrm{MAC}} = T_{\mathrm{RTS}} + T_{\mathrm{CTS}} + 3T_{\mathrm{SIFS}}$, where T_{RTS} and T_{CTS} are the time consumed on RTS and CTS, respectively, and

T_{SIFS} is the SIFS period. And, for each path failure, the delay due to packet retransmission is $N_R(t_d + T_{\mathrm{MAC}})$, where N_R is the MAC retransmission count, and t_d is the time for each data packet transmission. Combining the time consumed on both the MAC and routing layers, the delay introduced by path failure can be written as

$$\begin{aligned}\Phi_{\mathrm{A}} &= \Phi^d \Omega_{\mathrm{A}} T + \frac{T N_p \Omega_{\mathrm{A}} (t_r + T_{\mathrm{MAC}})(\hat{\mathcal{H}} + 1)}{2} \\ &\quad + T N_p \Omega_{\mathrm{A}} N_R (t_d + T_{\mathrm{MAC}}) + T \Omega_{\mathrm{A}} T_{\mathrm{MAC}} \hat{\mathcal{H}} \qquad (39) \\ \Phi_{\mathrm{C}} &= \Phi^d \Omega_{\mathrm{C}} T + T N_p \Omega_{\mathrm{C}} (t_h + T_{\mathrm{MAC}}) \hat{\mathcal{I}} \\ &\quad + T \Omega_{\mathrm{C}} N_R (t_d + T_{\mathrm{MAC}}) + T \Omega_{\mathrm{C}} T_{\mathrm{MAC}} \hat{\mathcal{H}}. \qquad (40)\end{aligned}$$

Comparison of terms in (39) and (40) shows that, whenever route discovery frequency $\Omega_{\mathrm{C}} < \Omega_{\mathrm{A}}$, terms 1, 3 and 4 are less for CA-AOMDV than for AOMDV. Term 3 is also advantaged in CA-AOMDV because it does not have the multiplicative N_p term. In term 2, however, the relative values depend on the actual value of $\hat{\mathcal{I}}$, which has been defined as $\hat{\mathcal{I}} < \hat{\mathcal{H}}$, the relative values of t_r and t_h and the relative values of Ω_{C} and Ω_{A}. Generally, AOMDV spends time on repairing path failure, which is preempted by adopting a handoff scheme in CA-AOMDV. The absence of handoff in AOMDV also increases the MAC delay due to packet retransmission in the event of path failure.

When IEEE 802.11 DCF is employed, we should also consider the throughput degradation due to channel access contention. Based on a random network traffic model, the maximum number of nodes in the network which might be involved in packet relaying is

$$N_a = \begin{cases} \hat{\mathcal{H}} C, & \hat{\mathcal{H}} C < N; \\ N, & \hat{\mathcal{H}} C \geq N. \end{cases} \qquad (41)$$

Then, the probability that a node has packets to transmit is N_a/N. In networks with IEEE 802.11 DCF, nodes within each other's transmission ranges cannot transmit at the same time. Under heavy traffic conditions (every node always has packets to transmit), 802.11 DCF provides long term per packet fairness in single-hop networks [33], thus each node in the shared wireless channel has a probability of $1/(n+1)$ of occupying the channel, where n is the number of node neighbors. Combining this with the probability that a node has packets to transmit, the average node transmission probability is $N_a/(n+1)N$. For a transmitting node on an active path, the probability that it can occupy the channel, or the probability that the channel won't be occupied by any of its n neighbors, is

$$q = 1 - \frac{N_a n}{(n+1)N}. \qquad (42)$$

Because each node on a path suffers the same average throughput degradation due to channel access contention, the time available for data transmission in a path is $(T - \Phi)q$. The achievable packet delivery ratio is $\Psi = (T - \Phi)q/T$. For AOMDV and CA-AOMDV respectively, the packet delivery ratio in the network is

$$\Psi_{\mathrm{A}} = \frac{(T - \Phi_{\mathrm{A}})q}{T}, \;\; \Psi_{\mathrm{C}} = \frac{(T - \Phi_{\mathrm{C}})q}{T} \qquad (43)$$

where Φ_{A} and Φ_{C} are given in (39) and (40), respectively. Therefore, whenever $\Phi_{\mathrm{A}} > \Phi_{\mathrm{C}}$ the packet delivery ratio of CA-AOMDV will be greater than that of AOMDV.

6 Simulation Results

For simulations we used network simulator ns-2.34 [34], implementing the mobile-to-mobile channel as in [35], [36], Doppler frequency controlled by transmitter and receiver movements, "hello" packet interval of 1000 ms and physical layer parameters of the Lucent WaveLAN wireless network card [34], with the random waypoint [37] mobility model. Constant Bit Rate (CBR) sources are used with the IEEE 802.11 DCF MAC protocol.

6.1 Evaluation of ANFD in Routing

We evaluate the throughput performance of a single link under different ANFDs. The simulated network has an area of 1000m $\times$ 1000m, channel bandwidth of 2 Mb/s and 50s running time. Nodes A and B are placed 70m apart, moving in parallel directions. Node A moves with a fixed speed of $v_A = 1$m/s, while node B moves with speeds of 1m/s, 1.5m/s, 2m/s, 2.5m/s, and 3m/s, respectively, with $\mu = 1, 1.5, 2, 2.5, 3$ accordingly. By changing the speed of node B, we change the ratio of their speeds, thus varying the ANFD value for the link according to (1). The data packets are 512 bytes, transmitted at a rate of 40 packets per second. The network throughput versus velocity ratio, μ, is shown in Fig. 6. Link throughput is inversely proportional to μ. With increased μ, node mobility is increased, thereby decreasing link ANFD. As expected, lower mobility achieves higher network throughput, so utilising the ANFD in the routing metric can help to improve network throughput.

6.2 Varying Node Mobility

We now compare AOMDV and CA-AOMDV with respect to node mobility. The simulated network areas were 2200 m $\times$ 600 m and 2800 m $\times$ 600 m, 2 Mb/s channel bandwidth, 100s running time, 100 uniformly distributed nodes moving at maximum speed in random directions with 20 connections. Maximum node speed was increased from 1 m/s to 10 m/s. The 512 byte CBR sources were fixed at 5 packets/s.

6.2.1 Throughput

Simulation results for network throughput are shown in Fig. 7. Throughput decreases with increased node mobility, with CA-AOMDV outperforming AOMDV, particularly in the mid-range mobilities, with significant performance increases realised. At 4 m/s, CA-AOMDV provides 25.5% and 12.2% improvements for the smaller

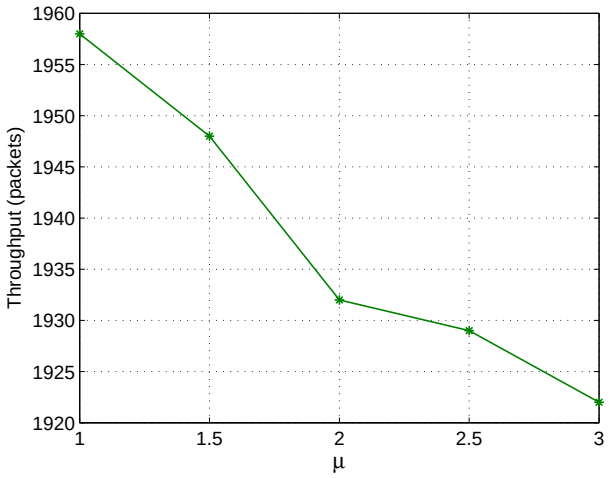

Fig. 6. Link throughput vs. μ, $\mu = v_B/v_A$, v_A is fixed at 1m/s, for communicating nodes, A and B, moving in parallel directions, separated by 70m, initially.

and larger networks, respectively. At extreme mobilities the throughput performances vary less and the advantages of CA-AOMDV are greater with smaller network area (shorter path lengths) as previously noted. At low mobilities, path characteristics vary less quickly and the advantages of handoff in CA-AOMDV are less. At high mobilities channel and path characteristics change rapidly, again mitigating handoff scheme advantages, and increasing signal strength prediction efficacy.

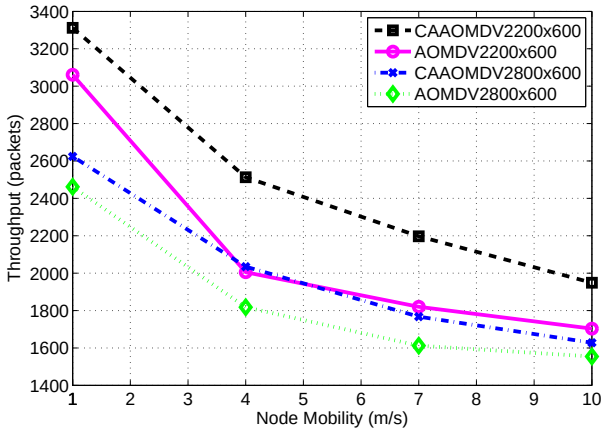

Fig. 7. Network throughput comparison between CA-AOMDV and AOMDV with increasing node mobility.

6.2.2 End-to-End Delay

Fig. 8 shows average packet transmission delay results. CA-AOMDV outperforms AOMDV, with 24% and 28% improvements at a velocity of 4 m/s, for the smaller and larger networks, respectively. At extreme mobilities the performances converge.

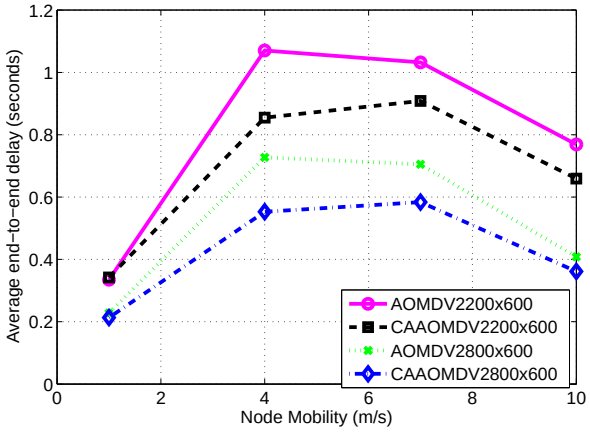

Fig. 8. Average end-to-end delay comparison between CA-AOMDV and AOMDV with increasing node mobility.

6.2.3 Normalized Routing Control Overhead

Normalized routing control overhead is the ratio of number of routing control packets to delivered data packets, as plotted in Fig. 9. Overhead for both protocols increases with increasing node mobility because the more quickly changing network topology increases routing update frequency. Except for extreme mobilities, CA-AOMDV maintains a lower routing overhead compared with AOMDV, with a 14% and 16% improvements at 4 m/s for the smaller and larger networks, respectively.

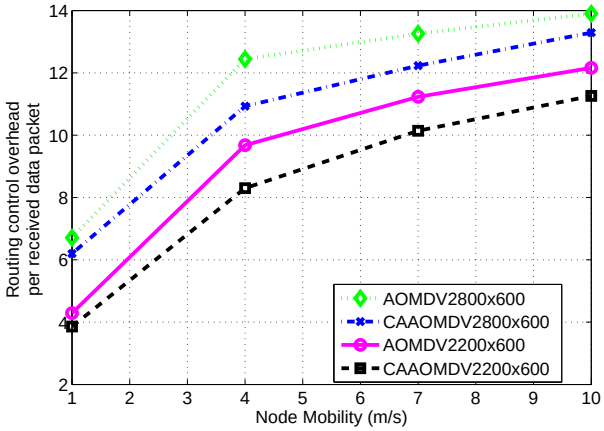

Fig. 9. Routing control overhead (normalized with respect to delivered data packets) comparison of CA-AOMDV and AOMDV with increasing node mobility.

6.3 Varying Traffic Load

To evaluate network traffic load performance we fixed maximum speed at 1 m/s, varying source packet rate from 5 to 40 packets/s. All other parameters were as in the previous section. Fig. 10 shows variation of packet delivery ratio (PDR) with increasing packet rate, while Fig. 11 shows variation of average end-to-end delay with increasing packet rate.

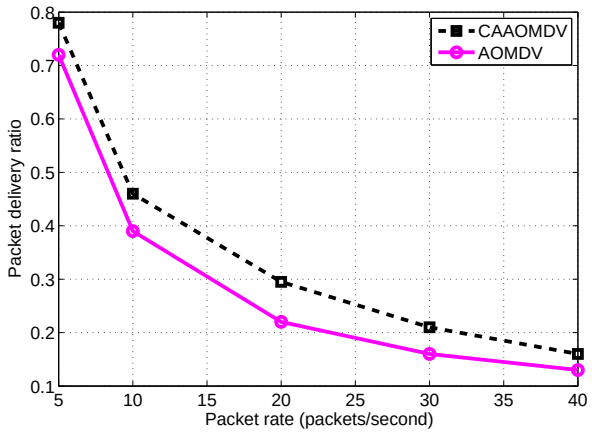

Fig. 10. Packet delivery ratio comparison between CA-AOMDV and AOMDV with increasing packet rate.

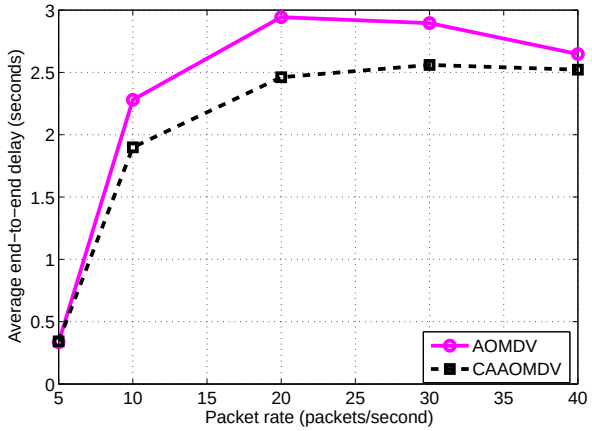

Fig. 11. Average end-to-end delay comparison between CA-AOMDV and AOMDV with increasing packet rate.

Both protocols have decreased PDR with increasing packet rate. For low traffic loads, increased packet rate prolongs the average end-to-end delay. After a certain point the packet delays decrease with increasing packet rate. The decrease of average end-to-end delay in Fig. 11 occurs because, at higher packet rate, more packets are dropped due to congestion. For both PDR and average end-to-end delay, CA-AOMDV outperforms AOMDV. For a packet rate of 20 packets/second, there is a 34.1% improvement of packet delivery ratio and 18.7% improvement of the average end-to-end delay.

6.4 Validation of the Theoretical Model

In this section we validate the theoretical analysis from Section 5. The network had 80 nodes, 10 connections, 1Mb/s channel bandwidth, 1000 byte packets at 4 packets/s, running for 300 seconds. Average link lifetimes were varied by changing network size, for a fixed number of nodes, and the node velocities for a fixed transmission range. Average path lifetime is increased from 8s to 50s.

The theoretical and simulated routing control overhead results are shown in Fig. 12 and match quite well. For short path lifetimes, the theoretical values are higher than the simulation values because the average distance between nodes is long and/or they are moving quickly. Under such conditions, long paths are difficult to establish. Thus, the established paths in the simulated network are shorter than those in the theoretical model, and the probability of a path breaking in the simulated network is lower than in theory. For longer path lifetimes, the theoretical values are lower than the simulation values, which may be due to overhead introduced by interference and packet collisions. CA-AOMDV performs better than AOMDV for both the simulated and theoretical results, as expected.

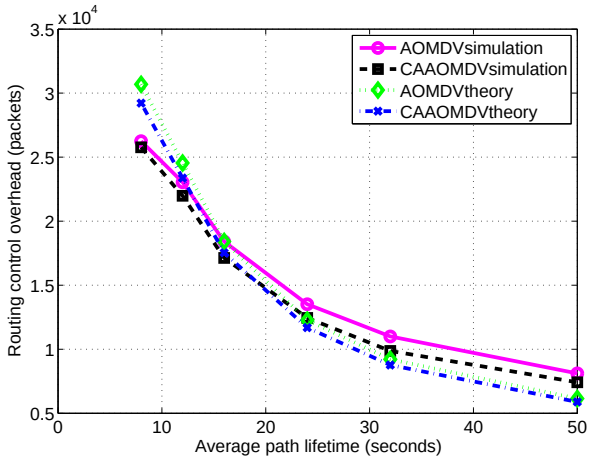

Fig. 12. Routing control overhead comparison of theoretical and simulated results with increasing average path lifetime. Theoretical values evaluated from (36) and (37).

CA-AOMDV outperforms AOMDV for both theoretical and simulated packet delivery ratio as shown in Fig. 13. Although the theoretical results follow the same trend as the simulated results, the former are always higher, especially for lower average path lifetimes. The difference is due to interference and packet collisions. In an adverse environment, with high frequency of broken paths, packet drop rate and number of packet retransmissions are relatively high, raising the amount of interference and number of collisions, incurring greater congestion. The packet drop rate can increase dramatically during congestion. As for previous results with respect to low and high mobility, the PDR performance of AOMDV and CA-AOMDV converge for low and high average path lifetimes.

7 Conclusion

A channel-based routing metric is proposed which utilizes the average non-fading duration, combined with hop-count, to select stable links. A channel adaptive routing protocol, CA-AOMDV, extending AOMDV, based on the proposed routing metric, is introduced.

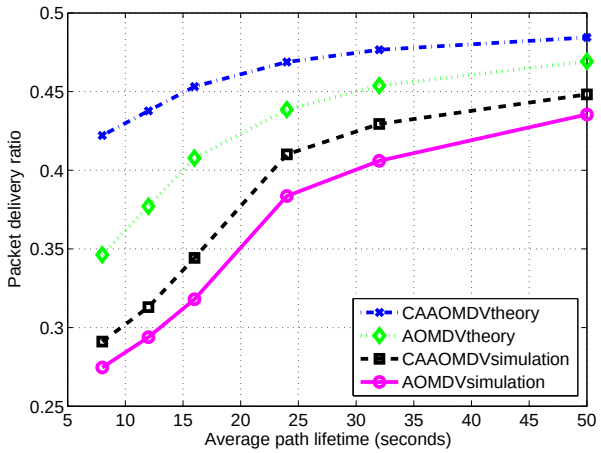

Fig. 13. Packet delivery ratio comparison between theoretical and simulated results with increasing average path lifetime. Theoretical values evaluated from (43).

During path maintenance, predicted signal strength and channel average fading duration are combined with handoff to combat channel fading and improve channel utilization. A new theoretical expression for the lifetime of the multiple reusable path system used in CA-AOMDV is derived. Theoretical expressions for routing control overhead and packet delivery ratio also provide detailed insights into the differences between the two protocols. Theoretical analysis and simulation results show that CA-AOMDV outperforms AOMDV in practical transmission environments.

REFERENCES

[1] W. C. Jakes, *Microwave mobile communications*, 2nd, Ed. WILEY INTERSCIENCE, 2001.
[2] G. L. Stuber, *Principles of mobile communication*, 2nd ed. Kluwer Academic Publishers, 2001.
[3] S. Jain and S. R. Das, "Exploiting path diversity in the link layer in wireless ad hoc networks," *WoWMoM*, pp. 22–30, Jun 2005.
[4] P. Pham, S. Perreau, and A. Jayasuriya, "New cross-layer design approach to ad hoc networks under Rayleigh fading," *JSAC*, vol. 23, no. 1, pp. 28–39, Jan 2005.
[5] C. Toh, "Associativity-based routing for ad-hoc mobile networks," *Personal Comms.*, vol. 4, pp. 103–139, Nov 1997.
[6] H. Zhang and Y. N. Dong, "Mobility prediction model based link stability metric for wireless ad hoc networks," *WCNMC*, pp. 1–14, Sep 2006.
[7] O. Tickoo, S. Raghunath, and S. Kalyanaraman, "Route fragility: A novel metric for route selection in mobile ad hoc networks," *ICON*, pp. 537–542, Sep 2003.
[8] S. Biswas and R. Morris, "ExOR: opportunistic multi-hop routing for wireless networks," *SIGCOMM*, vol. 35, no. 4, pp. 133–144, 2005.
[9] R. Dube, C. Rais, K. Y. Wang, and S. K. Tripathi, "signal stability-based adaptive routing (SSA) for ad hoc networks," *Personal Comms.*, vol. 4, no. 1, pp. 36–45, Feb 1997.
[10] M. Park, J. Andrews, and S. Nettles, "Wireless channel-aware ad hoc cross-layer protocol with multi-route path selection diversity," *VTC Fall*, vol. 4, pp. 2197–2201, Oct 2003.
[11] X. Lin, Y. K. Kwok, and V. K. N. Lau, "RICA: A receiver-initiated approach for channel-adaptive on-demand routing in ad hoc mobile computing networks," *ICDCS*, pp. 84–91, Jul 2002.
[12] B. Awerbuch, D. Holer, and H. Rubens, "High throughput route selection in multi-rate ad hoc wireless networks," *WONS*, pp. 251–269, Mar 2004.
[13] S. Zhao, Z. Wu, A. Acharya, and D. Raychaudhuri, "PARMA: a PHY/MAC aware routing metric for ad-hoc wireless networks with multi-rate radios," *WoWMoM*, pp. 286–292, Jun 2005.
[14] M. R. Souryal, B. R. Vojcic, and R. L. Pickholtz, "Information efficiency of multihop packet radio networks with channel-adaptive routing," *JSAC*, vol. 23, no. 1, pp. 40–50, Jan 2005.
[15] M. K. Marina and S. R. Das, "On-demand Multipath Distance Vector Routing in ad hoc networks," *ICNP*, pp. 14–23, Nov 2001.
[16] C. E. Perkins and E. M. Royer, "Ad-hoc on-demand distance vector routing," *WMCSA*, pp. 90–100, Feb 1999.
[17] A. S. Akki, "Statistical properties of mobile-to-mobile land communication channel," *Trans. VT*, vol. 43, no. 4, pp. 826–831, Nov 1994.
[18] M. Haenggi, "Routing in ad hoc networks - a wireless perspective," *BroadNets*, pp. 652–660, Dec 2004.
[19] A. Savvides, C. C. Han, and M. Srivastava, "Dynamic fine-grained localization in ad-hoc networks of sensors," *ACM MOBICOM*, pp. 166–179, May 2001.
[20] D. Niculescu and B. Nath, "Ad hoc positioning system (APS)," *GLOBECOM*, pp. 2926–2931, Nov 2001.
[21] C. Savarese, J. M. Rabaey, and J. Beutel, "Locationing in distributed ad-hoc wireless sensor networks," *ICASSP*, vol. 4, pp. 2037–2040, Dec 2001.
[22] D. Niculescu and B. Nath, "Ad hoc positioning system (APS) using AoA," *INFOCOM*, pp. 1734–1743, Apr 2003.
[23] N. Priyantha, A. Miu, H. Balakrishnan, and S. Teller, "The cricket compass for context-aware mobile applications," *MOBICOM*, pp. 1–14, Jul 2001.
[24] A. B. Mnaouer, L. Chen, C. H. Foh, and J. W. Tantra, "OPHMR: an optimized polymorphic hybrid multicast routing protocol for MANET," *Trans Mobile Comp*, vol. 5, no. 6, pp. 503–514, May 2007.
[25] Z. Zaidi and B. Mark, "A mobility tracking model for wireless ad hoc networks," *WCNC*, pp. 1790–1795, Mar 2003.
[26] L. L. Scharf, *Statistical Signal Processing: Detection, Estimation, and Time Series Analysis*. Addison-Wesley, 1991.
[27] W. Su and M. Gerla, "IPv6 flow handoff in ad hoc wireless networks using mobility prediction," *GLOBECOM*, vol. 1a, pp. 271–275, Dec 1999.
[28] T. Goff, N. Abu-Ghazaleh, D. Phatak, and R. Kahvecioglu, "Preemptive routing in ad hoc networks," *ICMCN*, pp. 43–52, Jul 2001.
[29] J. Bicket, D. Aguayo, S. Biswas, and R. Morris, "Architecture and evaluation of an unplanned 802.11b mesh network," *MobiCom*, pp. 31–42, Aug 2005.
[30] S. Panichpapiboon, G. Ferrari, and O. K. Tonguz, "Optimal transmit power in wireless sensor networks," *Trans Mobile Comp*, vol. 5, no. 10, pp. 1432–1447, Oct 2006.
[31] A. Nasipuri and S. R. Das, "On-demand multipath routing for mobile ad hoc networks," *CCCN*, pp. 64–70, Oct 1999.
[32] A. S. Akki and F. Haber, "A statistical model of mobile-to-mobile land communication channel," *Trans. VT*, vol. VT-35, pp. 2–10, Feb 1986.
[33] M. Heusse, F. Rousseau, G. Berger-Sabbatel, and A. Duda, "Performance Anomaly of 802.11b," *INFOCOM*, vol. 2, pp. 836–843, Mar 2003.
[34] "http://www.isi.edu/nsnam/ns/."
[35] C. S. Patel, G. L. Stuber, and T. G. Pratt, "Simulation of Rayleigh-faded mobile-to-mobile communication channels," *Trans. Comm.*, vol. 53, no. 11, pp. 1876–1884, 2005.
[36] R. J. Punnoose, P. V. Nikitin, and D. D. Stancil, "Efficient simulation of ricean fading within a packet simulator," *VTC*, vol. 2, pp. 764–767, Sep 2000.
[37] J. Broch et al, "A performance comparison of multi-hop wireless adhoc network routing protocols," *MobiCom*, pp. 85–97, Oct 1998.

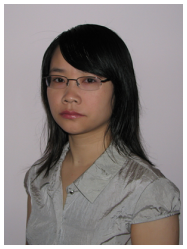

Xiaoqin Chen received the B.E. degree in Electrical and Electronic Engineering from Tianjin University, China in 1996, and the PhD degree in Wireless Communications Engineering from the Australian National University, Australia in 2009, respectively. She was a research fellow at Queensland University of Technology, and is now a system engineer at Star Intellect Pty Ltd. Her research interests include cross-layer design, channel-adaptive routing and MAC protocol design, radio resource management, packet scheduling, link adaptation and network optimisation for wireless networks.

Haley Jones received the B.E.(hons) degree in Electrical and Electronic Engineering and the B.Sc. degree from the University of Adelaide, Australia in 1992 and 1995, respectively. She received the PhD degree in Telecommunications Engineering from the Australian National University, Canberra, Australia in Oct. 2002. She has been an academic in the College of Engineering & Computer Science, The Australian National University, since January 2002. Dr Jones' previous experience includes time in industry and working on speech coding with the Cooperative Research Centre for Robust and Adaptive systems from 1993 to 1999. Her research interests have included wireless channel modelling, beamforming, channel and topology issues in MANETs. She has recently branched out into sustainable systems with a particular emphasis on the cradle-to-cradle paradigm and its application to sustainable manufacturing.

Dhammika Jayalath received the BSc degree in Electronics and Telecommunications Engineering from University of Moratuwa, Sri Lanka, and the MEng degree in Telecommunications from the Asian Institute of Technology, Thailand. He received the PhD degree in Wireless Communications from Monash University, Australia in 2002. He was a fellow at the Australian National University and a senior researcher at the National CT Australia. His research interests fall in the general areas of communications and signal processing. and he has published significantly in these areas. His current research interests include cooperative communications, cognitive radios, statistical signal processing and multiuser communications. He is currently serving as the Chair of the Signal Processing and Communications Chapter of the IEEE Queensland Section. He is a senior member of the IEEE.